図1　血管性認知症モデルの記憶障害

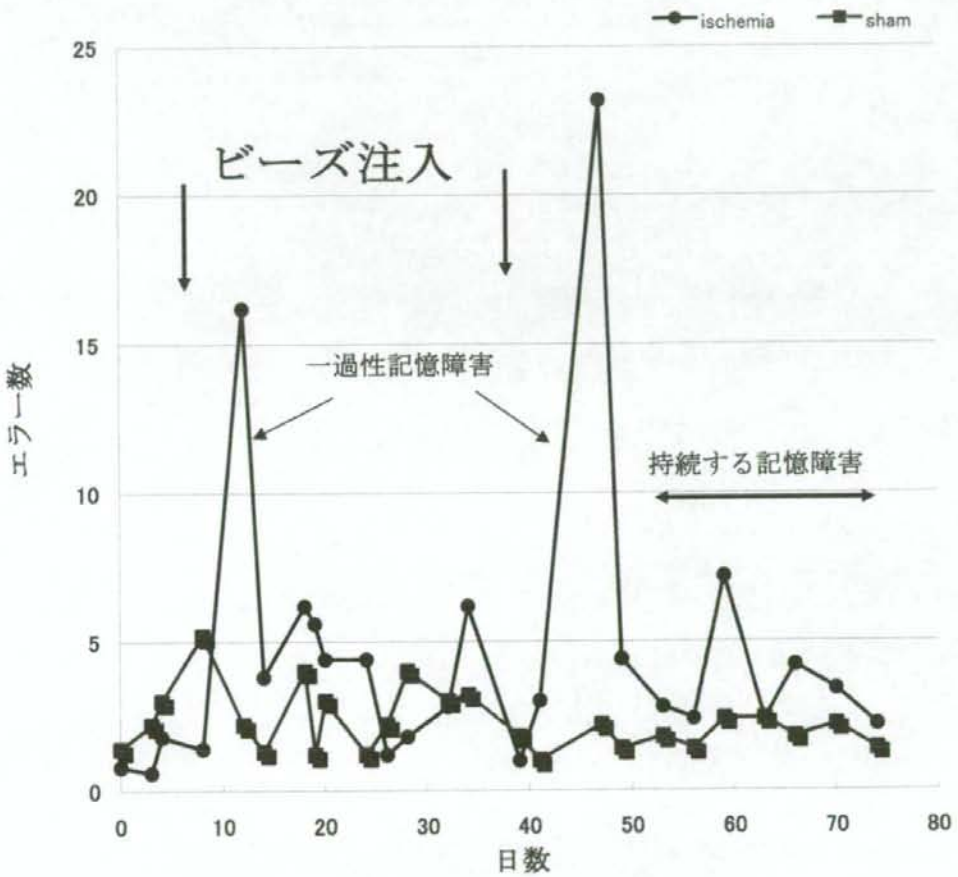

図2　MRI虚血病変の病理像

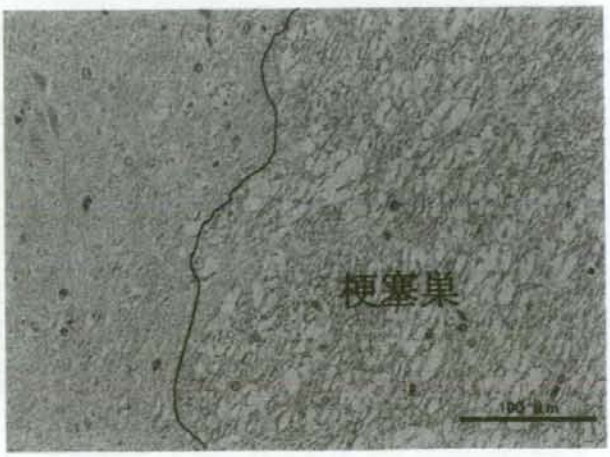

厚生労働科学研究費補助金（長寿科学総合研究事業）
分担研究報告書

霊長類血管性認知症モデル動物の確立とMRI画像解析

研究分担者　冨本秀和　三重大学大学院医学系研究科　神経病態内科学　教授

研究要旨
カニクイザルを用い、マイクロビーズを両側内頚動脈から注入する血管性認知症モデル動物を作製しMRI画像を評価した。MRI画像上大脳半球に虚血による組織障害を検出した。

A．研究目的

血管病変によって認知機能低下する機序は、1．視床など認知機能に重要な部位が小梗塞によって戦略的に傷害される（strategic single infarct dementia）、2．びまん性白質病変によって神経ネットワーク機能が障害される、3．大血管病変によって広汎に脳機能が傷害される、4．皮質微小梗塞（Cortical microinfarct；CMI）によって皮質神経機能が低下するなどに大別されている。従って、これらの病変の組み合わせで生じる病態は多様であり、血管性認知症は異質な病態を含む症候群である。特にCMIは近年、アルツハイマー病やアミロイド血管症との関連でその重要性が指摘されており、認知機能障害と強く相関することが神経病理学的疫学調査の結果から示されている。本研究は大脳皮質、穿通枝領域などに微小梗塞を作成し、血管性認知症の霊長類モデルを作成することを目標とする。当分担研究者は頭部MRI画像の解析を通して、血管病変の進展過程を明らかにする。

B．研究方法

モデル動物の作製は独立行政法人医薬基盤研究所霊長類医科学研究センターにて実施した。カニクイザルを用いたモデル動物の作製を7頭について行った。モデル動物は名古屋市立大学の間瀬光人の協力によって作製した。また、社団法人予防衛生協会の研究支援を受けた。

具体的には、X線透視下セルジンガー法により右大腿動脈にガイディングカテーテルを挿入して脳血管撮影を行った。この後、このガイディングカテーテルを総頚動脈に留置し，内腔にマイクロカテーテルを通して先端を内頚動脈のサイフォン部手前に置き、虚血群では滅菌された50 micronのマイクロビーズを、偽手術群では生理食塩水を両側に注入した。両群とも、一ヶ月の後に同様の処置を追加した。

7匹の実験条件は下記のごとくである。

＃1：一側330（計660）
　2：一側660（計1320）
　3：一側1400（計2800）
　4：一側2250（計4500）
　5：一側2800（計5600）
　6：生理食塩水
　7：同上

各動物につき処置前、術後3時間、1ヶ月、追加手術（1ヶ月）後3時間、2ヶ月、3-4ヶ月後の時系列で頭部MRI検査を行った。用いたシークエンスはT1-3D画像，T2WI, Proton density WI, DWI, PWI, 拡散Tensor, T2*, MRAの各項目である。

（倫理面への配慮）

本研究で用いる疾患モデル動物については、所属研究機関の各専門委員会の承認を受けて行った。また、疾患モデル動物の処置については霊長類医科学研究センターの規定に従い、動物愛護精神にのっとり慎重に行った。

C．研究結果

撮像条件で最も恒常的な変化はT2強調画像、T2*で認められた。DWI，MRAでは変化を認めなかった。以下、各個体の陽性所見を提示する。

＃1．追加手術3日後　左島皮質、左半卵円中心前方部にT2高輝度域が一過性に出現したが、2-4か月後には消失していた。T2*では低輝度点状病変が1か月後～追加手術3日後に認められた。4ヶ月後脳室拡大はなかったが、軽度の皮質萎縮を認めた。

＃2．1か月後、左基底核にT2高輝度、追加手術3日後両側基底核にT2高輝度の点状病変を数か所認めた。また、初回術後から追加手術3日後まで、基底核から放線冠の

T2*低輝度点状病変が出現していた。４ヶ月後、脳室拡大・皮質の中等度萎縮を認めた。
＃３．初回手術７日後に右前頭皮質、半卵円中心にＴ２高輝度域が散在したが、１ヶ月後には消失した。T2*低輝度点状病変は経過を通して認めなかった。追加手術3日後に左基底核、1ヵ月後に左半卵円中心にT2 高輝度点状病変を認めた。4ヶ月後　軽度の脳室拡大、脳溝の狭小化を認めた。
＃４．T2 高輝度域は明らかなものは認めなかった。追加手術３日後から３ヶ月まで、T2*低輝度点状病変が両側基底核に分布した。４ヶ月後軽度の皮質萎縮を認めた。
＃５．初回術後3時間で左ACA/MCA の浅在性境界領域に一致して、正常構造である皮質深層の高輝度帯の消失を認めた。3日後には、左優位にACA/MCA境界領域、半卵円中心、放線冠にT2 高輝病変が出現し、経過とともに徐々に退縮したが、４ヶ月までで遺残した。T2*低輝度点状病変は、初回術後３日から2.5ヶ月まで左前角周囲を中心に両側基底核、大脳皮質の皮髄境界直下に多発していた。粗大病変が存在する左前頭葉では、術後１０日のＰＷＩで脳血流の低下を認めた。４ヶ月になると脳室、脳溝が拡大した。
＃６．再手術10日後、左放線冠にT2*低輝度域を認めた。
＃７．異常なし。

D. 考察
　偽手術群ではT2高輝度病変、脳萎縮は認めなかった。一方、T2*低輝度点状病変は偽手術群でも認めることから、微小出血以外に一部は小血管を直接描出している可能性がある。＃５は病変の分布が最も広汎かつ高度であり、その領域は深部および浅在性の境界領域梗塞に一致していた。境界領域梗塞の病態には血行動態性機序のほか、最近では塞栓性機序の関与が指摘されているが、今回の結果はその仮説を実験的に裏付けるものであった。
　本研究ではマイクロビーズの数に相関して微小梗塞、微小出血が急性期から境界領域を中心に観察され、４ヶ月後に脳萎縮を認めた。病理・行動評価の結果と併せて判断する必要があるものの、頭部MRの結果は血管性認知症のモデルとしての可能性が示すものであった。

F．健康危険情報
なし

E．結論
　マイクロビーズの動脈内投与による組織障害がMR画像で検出可能であった。今後、病変の進展と認知機能の相関について明らかにする必要がある。

G．研究発表
1．論文発表
なし

2．学会発表
なし

H．知的財産権の出願・登録状況
（予定を含む。）

1. 特許取得
なし

2. 実用新案登録
なし

3.その他
なし

研究協力者
眞木崇州
京都大学　脳病態生理学講座
大学院生

間瀬光人
名古屋市立大学大学院医学研究科
社会復帰医学講座
神経機能回復学
准教授

別紙４

研究成果の刊行に関する一覧表

書籍

著者氏名	論文タイトル名	書籍全体の編集者名	書　籍　名	出版社名	出版地	出版年	ページ
武田和也、吉崎嘉一、田平　武	認知症モデルマウス	日本基礎老化学会編	老化・老年病研究のための動物実験ガイドブック	アドスリー	東京	2008	218-223
田平　武	記憶の加齢変化とアンチエイジング	日本抗加齢医学会専門医・指導士認定委員会編	アンチエイジング医学の基礎と臨床	Medical View社	東京	2008	124-125
田平　武	加齢性脳神経疾患とアンチエイジング	日本抗加齢医学会専門医・指導士認定委員会編	アンチエイジング医学の基礎と臨床	Medical View社	東京	2008	131-132
田平　武	老化とストレス、うつ	日本抗加齢医学会専門医・指導士認定委員会編	アンチエイジング医学の基礎と臨床	Medical View社	東京	2008	308-309
田平　武	脳機能とアンチエイジング	日本抗加齢医学会専門医・指導士認定委員会編	アンチエイジング医学の基礎と臨床	Medical View社	東京	2008	356-357

雑誌

発表者氏名	論文タイトル名	発表誌名	巻号	ページ	出版年
Wang, J., Hara, H., Makifuchi, T., Tabira, T.	Development and characterization of a TAPIR-like mouse monoclonal antibody to Aβ.	**J Alzheim Dis**	14	161-73	2008
Liu, H., Wang, J., Sekiyama, A., Tabira T.	Juzen-taiho-to, an Herbal Medicine, Activates and Enhances Phagocytosis in Microglia/ Macrophages.	**Tohoku J Exp Med**	215	43-54	2008
Yoshizaki K, Adachi K, Kataoka S, Watanabe A, Tabira T, Takahashi K, Wakita H.	Chronic cerebral hypoperfusion induced by right unilateral common carotid artery occlusion causes delayed white matter lesions and cognitive impairment in adult	**Exp Neurol**	210	585-91	2008
Ma L, Ohyagi Y, Miyoshi K, Sakae N, Motomura K, Taniwaki T, Furuya H, Takeda K, Tabira T, Kira J.	Increase in p53 Protein Levels by Presenilin 1 Gene Mutations and its Inhibition by Secretase Inhibitors.	**J Alzheimers Dis**	16(3)	565-75	2009

Miyoshi K, Ohyagi Y, Sakae N, Motomura K, Ma L, Taniwaki T, Furuya H, Tabira T, Kira J.	Enhancement of activation of caspases by presenilin 1 gene mutations and its inhibition by secretase inhibitors.	**J Alzheimers Dis**	16(3)	551-64	2009
Sakurai F, Nakamura S, Akitomo K, Shibata H, Terao K, Kawabata K, Hayakawa T, Mizuguchi H.	Transduction properties of adenovirus serotype 35 vectors after intravenous administration into nonhuman primates.	**Mol Ther**	16(4)	726-33	2008
Suzuki T, Sakurai F, Nakamura S, Kouyama E, Kawabata K, Kondoh M, Yagi K, Mizuguchi H.	miR-122a-regulated expression of a suicide gene prevents hepatotoxicity without altering antitumor effects in suicide gene therapy.	**Mol Ther**	16(10)	1719-26	2008

Journal of Alzheimer's Disease 14 (2008) 161–173
IOS Press

Development and Characterization of a TAPIR-Like Mouse Monoclonal Antibody to Amyloid-β

Jun Wang[a,b], Hideo Hara[a], Takao Makifuchi[c] and Takeshi Tabira[a,*]
[a]*Department of Vascular Dementia Research, National Institute for Longevity Sciences, National Center for Geriatrics and Gerontology, 36-3 Genko, Morioka, Obu, Aichi 474-8511, Japan*
[b]*Department of Neurology, 1st Affiliated Hospital, China Medical University, 155 North Nanjing Street, Shenyang 110001, P.R. China*
[c]*Department of Clinical Research, NHO Saigata National Hospital, 468-1 Saigata, Oogata, Jouetsu, Niigata 949-3193, Japan*

Communicated by Akihiko Takashima

Abstract. Tissue amyloid plaque immuno-reactive (TAPIR) antibody was better related to the effect of immunotherapy in Alzheimer's disease (AD) than ELISA antibody. Here we used a hybridoma technique to develop a TAPIR-like anti-human amyloid-β (Aβ) mouse monoclonal antibody. The obtained monoclonal antibody, 3.4A10, was an IgG2b isotype and recognized N-terminal portion of Aβ_{1-42} without binding denatured or native amyloid-β protein precursor. It had higher affinity to Aβ_{1-42} than to Aβ_{1-40} by Biacore affinity analysis and stained preferably the peripheral part of senile plaques and recognized the plaque core less than 4G8. It inhibited the Aβ_{1-42} fibril formation as well as degraded pre-aggregated Aβ_{1-42} peptide in a thioflavin T fluorescence spectrophotometry assay. The *in vivo* studies showed that 3.4A10 treatment decreased amyloid burden compared to the control group and significantly reduced Aβ_{42} levels rather than Aβ_{40} levels in brain lysates as well as the Aβ*56 oligomer (12mer) in TBS fraction of the brain lysates. 3.4A10 entered brain and decorated some plaques, which is surrounded by more Iba1-positive microglia. 3.4A10 therapy did not induce lymphocytic infiltration and obvious increase in microhemorrhage. We conclude that 3.4A10 is a TAPIR-like anti-human amyloid monoclonal antibody, and has a potential of therapeutic application for AD.

Keywords: Alzheimer's disease, immunotherapy, TAPIR-like anti-amyloid antibody

INTRODUCTION

Alzheimer's disease (AD) is the most common dementia in the elderly population. It has been estimated that up to 5% of the population older than 65 years is affected by AD [3] and the prevalence doubles approximately every 5 years beyond age 65 [4]. AD is a chronic neurodegenerative disorder that is characterized by progressive disturbances of cognitive functions including memory, judgment, language and so on clinically, and selective neuron and synapse losses, extracellular senile plaques containing amyloid-β peptide (Aβ) deposits as well as intraneuronal neurofibrillary tangles pathologically [4,22,28]. Although there is no curable treatment for AD, based on the growing understanding of the pathogenesis, several novel therapeutic strategies are being developed and Aβ immunotherapy is one of the potential methods [13]. Active and passive Aβ immunotherapies can reduce AD-like pathology and improve cognitive performance in animal models of the

*Corresponding author: Takeshi Tabira, National Institute for Longevity Sciences, National Center for Geriatrics and Gerontology, 36-3 Genko, Morioka, Obu, Aichi 474-8511, Japan. Tel.: +81 562 45 0183; Fax: +81 562 45 0184; E-mail: tabira@nils.go.jp.

ISSN 1387-2877/08/$17.00

disease [1,5,8,11,14,19,20,27] and potentially in AD patients [7,10]. Due to the side effects (meningoencephalitis) of the active immunization in a human trial and reduced response to active vaccination in the elderly [23,24], passive administration of anti-Aβ antibodies might be a more plausible approach. Hock and colleagues suggested that tissue amyloid plaque immunoreactive (TAPIR) antibodies were corresponding to the slower cognitive decline in AD patients who received active vaccination [10]. In this study, we developed a TAPIR-like anti-human Aβ monoclonal mouse antibody by a hybridoma technique and characterized it in vitro and also evaluated its therapeutic effects in 18 months old Tg2576 mice.

MATERIALS AND METHODS

Animals

Female BALB/c mice were purchased from Central Science Company (Nagoya, Japan) and amyloid-β protein precursor (AβPP) transgenic (Tg2576) mice were purchased from Taconic Farms (Germantown, NY, USA). They were housed in plastic cages and received food (CE2, Clea Japan Inc., Tokyo, Japan) and water *ad libitum*, and were maintained on a 12/12 hours light-dark cycle. All experiments were performed under the guidelines for Animal Experiments of National Center for Geriatrics and Gerontology and approval of the institute's ethical committee for animal experiment.

Antibodies

The antibodies used in this study were listed as follows: mouse anti-human Aβ monoclonal antibodies: 6E10 (recognizes 1–17 amino acid residues of Aβ, Chemicon International, Temecula, CA, USA), 4G8 (recognizes 17–24 amino acid residues of Aβ, Signet, Dedham, MA, USA) and 12F4 (recognizes C-terminus of $A\beta_{1-42}$, Signet); mouse anti-AβPP A4 monoclonal antibody 22C11 (Chemicon International); hamster anti-mouse CD3e monoclonal antibody and rat anti-mouse CD19 monoclonal antibody (BD Bioscience Pharmingen, San Jose, CA, USA); rabbit polyclonal anti-pan Aβ antibody (Biosource, Camarillo, CA, USA); rabbit anti-Iba1 polyclonal antibody (a gift from Dr. Imai at the National Institute of Neuroscience, NCNP); Cy3 conjugated mouse anti-glial fibrillary acidic protein (GFAP) monoclonal antibody, clone G-A-5 (Sigma-Aldrich, Saint Louis, MO, USA).

Immunization and establishment of hybridoma cell lines

The 6–8 weeks old female BALB/c mice were immunized with emulsion of 100 μl complete Freund's adjuvant (containing 1 mg/ml mycobacterium tuberculosis H37Ra, Difco Laboratories, Deteriot, MI, USA) and 100 μg $A\beta_{1-42}$ peptide (Peptide Institute, Inc., Osaka, Japan) in 100 μl PBS as previously described [27] and boosted with emulsion of 100 μl incomplete Freund's adjuvant (Difco Laboratories) and 100 μg $A\beta_{1-42}$ peptide in 100 μl PBS 2 weeks after the immunization. Just the day before the fusion, the mice received 100 μg $A\beta_{1-42}$ peptide in 100 μl PBS intraperitoneally. The spleens were harvested aseptically 4 weeks after the first immunization and the isolated splenocytes were fused to a myeloma cell line X63-Ag8.653 at 5:1 ratio in 50% w/v PEG (Hybri-Max®, MW1450, Sigma-Aldrich). The cell suspension was added into the 96-well plates (Becton Dickinson Labware, Franklin Lakes, NJ, USA) at 100 μl/well. The hybridoma cells were selected by adding 100 μl culture medium containing 2×HAT (Hybri-Max®, Sigma-Aldrich) to each well two days after fusion. When the most growing wells demonstrated 10 to 25% confluence, 100 μl of culture medium from each well to be tested was used to detect positive clones by an ELISA screening assay. To get monoclonal antibodies, limiting dilution at 5 cells/ml in concentration was performed twice. To keep the cells growing in the low concentration, 10% fetal bovine serum (ICN Biomedicals, Aurora, OH, USA) and 10% hybridoma cloning factor (BioVeris, Gaithersburg, MD, USA) were added into the culture medium (RPMI medium 1640, Gibco®, Invitrogen, Grand Island, NY, USA). The cells were cultured in a humidified 37°C, 5% CO_2 incubator.

Hybridoma screening and antibody isotyping

The 96 well ELISA plates (Nunc-Immuno plate, Maxisorb surface, Roskilde, Denmark) were coated with 100 μl of 4 μg/ml $A\beta_{1-42}$ peptide in 55 mM $NaHCO_3$ solution (PH 9.0) overnight at 4°C. Plates were washed with 20 mM Tris-HCl, pH 7.4 containing 150 mM NaCl and 0.05% Tween20 (TBS-T) 2 times and blocked with 1% BSA and 2% normal goat serum in TBS-T (blocking buffer) for 1 hour at room temperature (RT). Plates were washed 2 times and incubated with 100 μl hybridoma culture medium for 2 hours at RT. Plates were washed 4 times and incubated with 100 μl goat anti-mouse IgG+IgM (H&L)-HRPO (American

Qualex, San Clemente, CA, USA) diluted 1:2000 in blocking buffer for 2 hours at RT. Plates were washed 4 times and added 100 μl SureBlue Reserve™ TMB Microwell Peroxidase substrate (KPL, Baltimore, MD, USA) and allowed to develop color in dark for 30 minutes at RT. The plates were read at 450 nm wave length by a microplate reader (model 550, Bio-Rad Laboratories, Hercules, CA, USA) after adding 100 μl TMB stop solution (KPL). The isotypes of the monoclonal antibodies were detected by a mouse immunoglobulin isotyping ELISA kit (BD Biosciences Pharmingen) according to the assay procedure of the product instruction.

Ascites development and antibody purification

0.5 ml pristane (Sigma-Aldrich) was administrated to 6–8 weeks old female BALB/c mice intraperitoneally one week before hybridoma injection. The hybridoma cells were washed with PBS twice to eliminate fetal bovine serum and suspended with PBS at 5×10^6 cells/ml. Each mouse received 2 ml hybridoma cell suspension intraperitoneally. The ascites was allowed to develop for 2 weeks. If there was no ascites developed, hybridoma cell suspension was administrated to the mice again. The ascites was drained every 3 days by a 16 G needle till no ascites was drained or the mice died. The ascites was centrifuged for 10 minutes at 1500 × g, RT. The supernatants were harvested and kept at 4°C till purification. The monoclonal antibody was purified by an Affi-Gel® Protein A MAPS® kit (Bio-Rad Laboratories) according to the product manual and under the monitor of an ÄKTA FPLC system (Amersham Biosciences AB, Uppsala, Sweden). The purified monoclonal antibody was dialyzed against PBS. After 4 times dialysis, the antibody was filtrated by 0.22 μm filter (MILLEX®-GV PVDF syringe driven filter unit, Millipore, Cork, Ireland) and the concentration was measured by a BCA™ protein assay kit (Pierce Biotechnology, Rockford, IL, USA) with pre-diluted bovine gamma globulin (Pierce Biotechnology) as the standard. For *in vivo* study, the endotoxin was removed by a ProteoSpin™ endotoxin removal kit (Norgen Biotek, Ontario, Canada) following the product manual.

In vitro characterization of the monoclonal antibody

Dot blot and western blot for detection of Aβ peptide fragments and AβPP fragments

Several Aβ peptide fragments were used. $A\beta_{1-28}$ and $A\beta_{34-42}$ were purchased from Sigma-Aldrich. $A\beta_{25-35}$, $A\beta_{1-40}$ and $A\beta_{1-42}$ were purchased from Peptide Institute. All the peptides were dissolved in DMSO at the concentration of 1mM. Then an aliquot of each peptide was diluted with PBS to the final concentration at 4 μg/ml. 100 μl of each peptide solution was added to 0.2 μm nitrocellulose transfer membrane (Whatman GmbH, Dassel, Germany) in a dot blot device (Bio-Rad Laboratories). Then the membrane was blocked by 5% skim milk in TBS for 30 minutes at RT. After a short wash with dH_2O, the membrane was incubated with primary antibodies (3.4A10, our anti-Aβ monoclonal antibody and 4G8) at 1 μg/ml in StartingBlocking™ T20 (TBS) blocking buffer (Pierce Biotechnology) for 1 hour at RT. The membrane was washed 3 times with TBS-T and incubated with goat anti-mouse IgG (H&L)-HRPO (American Qualex) diluted 1:2000 in blocking buffer for 1 hour at RT. After washing, the dots were visualized by a western lightning chemiluminescence reagent (PerkinElmer, Boston, MA, USA). For western blot, 100 ng of $A\beta_{1-28}$, $A\beta_{1-40}$ and $A\beta_{1-42}$ was loaded into 16.5% peptide SDS-PAGE gels (Bio-Rad Laboratories, Tokyo, Japan) and transferred onto 0.2 μm nitrocellulose membrane at 200 mA for 1 hour. The subsequent steps were the same as dot blot. sAβPPα, immature AβPP and mature AβPP were got from the lysate of wild type human AβPP-transfected human neuroblastoma SH-SY5Y cells (generous gift from Dr. K. Takeda). 10 μl of the cell lysate was loaded into 7.5% SDS-PAGE gels (Daiichi Pure Chemicals, Tokyo, Japan) and the bands were detected by 1 μg/ml 3.4A10 or 22C11 in blocking buffer and visualized as described above.

Staining of AβPP-transfected SH-SY5Y living cell

Human neuroblastoma SH-SY5Y cells were transfected with an expression plasmid encoding wild type human AβPP. Staining of the cell surface AβPP ectodomains was performed as previously described [9]. Briefly, the cells were incubated with 5 μg/ml 3.4A10, 6E10 or normal mouse IgG in culture medium at 4°C for 30 minutes. After brief washing with PBS, the cells were fixed in 4% paraformaldehyde for 15 minutes, blocked, stained with Alexa-594 labeled Donkey anti-mouse IgG (Molecular Probes, Eugene, OR, USA) at 1:500 dilution and counter-stained the nuclei with Hoechst 33342 (Molecular Probes).

Biacore epitope and affinity analysis

Freshly prepared 50 μg/ml $A\beta_{1-40}$ and $A\beta_{1-42}$ peptides in 10 mM sodium acetate buffer, pH 4.0 were immobilized to the CM5 sensor chips (Biacore AB, Uppsala, Sweden) according to the user manual. All analyses were run on a Biacore J system (Biacore AB). For the competitive epitope analysis, an $A\beta_{1-42}$ immobilized CM5 chip was firstly saturated with 200 μg/ml 3.4A10 in PBS for 5 minutes at a flow rate of 30 μl/min, then 20:1 ratio antibody mixtures (3.4A10:6E10, 4G8 or 12F4) was injected at the same flow rate for 3 minutes and the response levels of each cycle were recorded. For the affinity analysis, 3.4A10 at concentrations ranging from 100 nM to 500 nM in PBS was injected into $A\beta_{1-40}$ or $A\beta_{1-42}$ immobilized CM5 sensor chips at a flow rate of 30 μl/min for 5 minutes. Dissociation of bound antibody in PBS flow was followed for 3 minutes and the data were analyzed by BIAevaluation software (Biacore AB). The chips were regenerated with 50 mM NaOH at a flow rate of 30 μl/min for 2 minutes after each cycle.

Thioflavin T fluorescence spectrophotometry

To determine whether 3.4A10 can inhibit $A\beta_{1-42}$ aggregation and disaggregate pre-aggregated $A\beta_{1-42}$, the experiments were performed as described previously [29,30]. For the inhibition assay, the freshly prepared 25 mM $A\beta_{1-42}$ in PBS was incubated with 2.5 mM 3.4A10 in a final volume of 25 μl at 37°C for 1 week, and 1 ml of 5 mM thioflavin T (Sigma Aldrich Chemie Gmbh, Steinheim, Germany) in PBS was added to the system and fluorescence was measured using a fluorescence spectrophotometer (Model F-2500, Hitachi, Tokyo, Japan) at an excitation wavelength of 445 nm and an emission wavelength of 490 nm. For the disaggregation assay, 10 μl of 62.5 mM $A\beta_{1-42}$ was incubated in PBS at 37°C for 1 week and then 3.4A10 was added at the final concentration of 2.5 mM and the final volume is adjusted to 25 μl. The mixture was incubated for another 48 hours and 1 ml of 5 mM thioflavin T was added to the mixture and fluorescence was measured as described above. PBS without antibody was added for the control. These experiments were repeated 3 times and duplicated each time. The results were the means of three independent experiments and the percentage of the control was used as presentation.

Senile plaque staining

The frozen sections of AD patient brain (with the permission of the family for AD study) were fixed with 70% formic acid for 20 minutes at RT. After washing with TBS-T, the sections were incubated with 0.3% H_2O_2 in methanol for 30 minutes to block endogenous peroxidase. The sections were washed with TBS-T and then incubated with 1 μg/ml 3.4A10 or 4G8 in the blocking buffer (5% skim milk in TBS containing 0.4% Triton X-100 and 10% normal horse serum) for 1 hour at RT. The sections were washed with TBS-T, 1:500 biotinylated horse anti-mouse IgG (Vector Laboratories, Burlingame, CA, USA) was added to the sections and incubated at RT for 1 hour. After washing, the sections were stained with Avidin-HRP/DAB kit (Vector Laboratories). Senile plaques with or without the plaque core were counted, and the difference between 3.4A10 and 4G8 was compared.

Passive immunization with 3.4A10

3.4A10 was administrated to 18 months old female Tg2576 mice intraperitoneally at 10 mg/kg body weight weekly for 8 weeks ($n = 4$). The control group received PBS only ($n = 4$).

Immunohistochemistry

After 8 weeks treatment, the mice were anesthetized by inhalation of diethyl ether. After blood samples were taken from heart, the mice were sacrificed by cervical dislocation. The brains were removed and cut in half sagittally. The hemisphere from each mouse was fixed in 4% paraformaldehyde at 4°C over night. The brains then were washed with PBS and dehydrated with gradient concentration of sucrose, and embedded in O.C.T. (Sakura Finetechnical, Tokyo, Japan). The frozen sections were cut with a Leica CM 1850 cryostat microtome (Leica Microsystem Nussloch GmbH, Nussloch, Germany) at 9 μm in thickness. Sections were washed with PBS and incubated with blocking buffer (5% skim milk in TBS containing 0.4% Triton X-100 with 10% normal second antibody relevant animal serum) for 30 minutes at RT. Sections were then incubated at RT for 2 hours with the antibody indicated below, washed with TBS-T, incubated with relevant biotin conjugated second antibody for 2 hours at RT, washed with TBS-T again, and stained by the avidin-biotin HRP/DAB method. The primary antibody against CD3e and CD19 were used at 1 μg/ml. Aβ plaque-containing sections were stained with rabbit polyclonal anti-pan Aβ antibody at 1 μg/ml. The samples were counterstained with hematoxylin.

A quantitative analysis of amyloid burden was performed by using a Winroof software (version 5.7, Mitani, Fukui, Fukui Ken, Japan) in the whole cortex and

hippocampus. Aβ burden was expressed as the percentage of brain tissue occupied by Aβ deposits. Three immunolabeled sections were analyzed per mouse, and the average of the individual measurements was used to calculate group means.

Immunofluorescence staining

To prove peripherally administrated 3.4A10 had entered the brain, the brain sections were firstly stained with 1 μg/ml rabbit anti-pan Aβ antibody in blocking buffer (10% normal donkey serum and 2% bovine serum albumin in TBS) for 1 hour at RT following 30 minutes incubation with blocking buffer. After 3 time washes with TBS-T, the sections were incubated with 1:500 Alexa 594-labeled donkey anti-mouse IgG antibody and 1:500 Alexa 488-labeled donkey anti-rabbit IgG antibody (Molecular Probes) for 1 hour at RT. After washing, the fluorescence was observed by a Olympus IX70 microscope (Olympus, Tokyo, Japan) and recorded by a Nikon digital camera DXM1200F (Nikon, Tokyo, Japan).

To evaluate activation of microglia, the sections were stained with 1 μg/ml rabbit anti-microglia polyclonal antibody (Iba-1), the microglia and senile plaques were visualized with 1:500 Alexa 488-labeled donkey anti-rabbit IgG antibody and Alexa 594-labeled donkey anti-mouse IgG antibody and the images were recorded by a Zeiss LSM510 image system (version 2.3, Carl-Zeiss Co., Ltd, Tokyo, Japan). The numbers of microglia associated with 3.4A10 positive and negative plaques were counted, and the average cell number per plaque was compared. The astrocytes were stained by 1:500 Cy3-conjugated mouse anti-GFAP monoclonal antibody. The fluorescence was observed and recorded as described above.

Berlin blue staining

To detect the hemorrhagic lesion in the mouse brain sections, Berlin blue stain was used. Briefly, brain sections were stained in potassium ferrocyanide solution (2% potassium ferrocyanide: 2% Hydrochloric acid = 1 vol:1 vol; Muto Pure Chemicals Co., Ltd, Tokyo, Japan) for 30 minutes at RT. After washing in distilled water, sections were incubated in Kernechtrot stain solution (Muto Pure Chemicals) for 2 minutes. The positive blood vessel numbers were counted in 3 sections per mouse, and average of the individual measurements was used to calculate group means.

ELISA measurements for Aβ levels in brain tissue lysate

The samples for measurement of insoluble and soluble Aβ was prepared as previously reported [8,20]. The brain hemispheres of both therapeutic and control groups were homogenized with a homogenizer in 1 ml of TBS with complete protease inhibitor plus 20 μg/ml pepstatin A (Roche Diagnostics GmbH, Mannheim, Germany), then centrifuged at 100,000 g for 1 hour at 4°C using an Optima TLX ultracentrifuge (Beckman-Coulter, Fullerton, CA, USA). The pellets were homogenized in 1 ml of 2% SDS/TBS with complete protease inhibitor, then centrifuged at 100,000 g for 1 hour at 25°C following 15 minutes incubation at 37°C. The pellets (corresponding to insoluble fraction of Aβ peptides) were homogenized in 1 ml of 70% formic acid and centrifuged at 100,000 g for 1 hour. The supernatants were neutralized with 1 M Tris-HCl, pH 8.0 at 1:20 ratio. The samples were kept in −80°C. The Aβ levels of SDS-fraction and formic acid fraction were quantified with an Aβ ELISA kit (Wako Pure Chemicals Industries) according to the product instruction. The supernatants were diluted with standard dilution buffer at 1:2000 ($A\beta_{1-40}$) or 1:400 ($A\beta_{1-42}$). The obtained values were corrected with the wet weight of each brain hemisphere samples and expressed as nmol/g brain.

Western blot for detection of Aβ oligomers in TBS fraction of brain lysate

For analysis of Aβ oligomers in the soluble fraction of mouse brain lysate, 10 μl of each TBS fraction of soluble brain lysates was loaded to 15/25 SDS-PAGE gel (Daiichi Pure Chemicals) and transferred to 0.2 μm nitrocellulose membrane. The bands were detected with 6E10 at 1: 2000 dilution and HRP-conjugated goat anti-mouse IgG (H&L) at 1: 5000 dilution and visualized as described above. The size of the bands was determined by using Alpha Ease FC software (Alpha Innoteck, San Leandro, CA, USA) based on the molecular weight of the standard.

Statistic analysis

All results were expressed as the mean ± SD except mentioned otherwise. The difference of the two groups was analyzed with Student's t test.

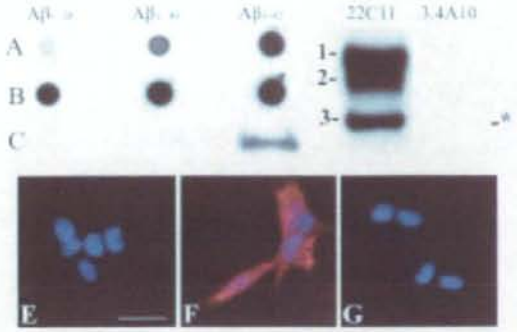

Fig. 1. 3.4A10 had higher affinity to $A\beta_{1-42}$ and did not bind native or denatured $A\beta$PP fragments. A) 400 ng of different $A\beta$ fragments were immobilized onto the nitrocellulose membrane, 1 μg/ml 3.4A10 or 4G8 was used to detect the dots. 3.4A10 recognized $A\beta_{1-28}$, $A\beta_{1-40}$ and $A\beta_{1-42}$ with an increasing signal density and did not bind $A\beta_{25-35}$ and $A\beta_{34-42}$ (data not shown). B) As a positive control, 4G8 recognized $A\beta_{1-28}$, $A\beta_{1-40}$ and $A\beta_{1-42}$ with an equal signal density. C) The western blot results showed that 3.4A10 recognized $A\beta_{1-42}$ monomer better than $A\beta_{1-40}$ monomer, and did not recognized $A\beta_{1-28}$ monomer. D) 3.4A10 did not recognize the denatured $sA\beta PP\alpha$, immature $A\beta$PP and mature $A\beta$PP separated on SDS-PAGE from cell lysate of human neuroblastoma SH-SY5Y cells transfected with wild type human $A\beta$PP, while as a positive control anti-$A\beta$PP N terminal-specific antibody 22C11 recognized these bands. 1, mature $A\beta$PP; 2, immature $A\beta$PP; 3, $sA\beta PP\alpha$; *, 100 kD. E) 3.4A10 did not bind native $A\beta$PP that was expressed on the surface of human neuroblastoma SH-SY5Y cell line transfected with wild type human $A\beta$PP by a living cell staining assay, 6E10 as a positive control (F), normal mouse IgG as a negative control (G). Bar = 20 μm; Blue, Hochst33342; Red, $A\beta$PP.

RESULTS

One IgG2b secretary hybridoma cell line was established

Each immunized spleen was used to perform one fusion. Totally 5 fusions were performed, and 8 anti-$A\beta$ antibody secretory hybridoma cell lines were detected by an ELISA screening assay. The monoclonal hybridoma cell line was established by twice limiting dilution. Then the isotype assay was performed. One cell line 3.4A10 was an IgG2b isotype, while others were an IgM isotype, and the clone 3.4A10 was investigated further in this study.

Results of in vitro studies

3.4A10 recognized N-terminal epitope of $A\beta_{1-42}$

To analyze the epitope of 3.4A10, the different $A\beta$ fragments were used firstly. Even though same amount of peptides was loaded to the membrane or SDS-PAGE gel, 3.4A10 had different signal density to the different peptide. Dot blot results showed that 3.4A10 recognized $A\beta_{1-28}$, $A\beta_{1-40}$ and $A\beta_{1-42}$ with an increasing signal density (Fig. 1A) and did not recognize $A\beta_{25-35}$ and $A\beta_{34-42}$ (data not shown), while as a positive control 4G8 recognized $A\beta_{1-28}$, $A\beta_{1-40}$ and $A\beta_{1-42}$ with a similar signal density (Fig. 1B). 3.4A10 bound $A\beta_{1-42}$ monomer with much higher density than $A\beta_{1-40}$monomer and did not recognize the $A\beta_{1-28}$ monomer on western blot (Fig. 1C). The epitope of 3.4A10 cannot be determined according to the data as above mentioned, to elucidate the epitope further, Biacore competitive epitope analysis was used. Biacore data showed that after saturation of $A\beta_{1-42}$ immobilized CM5 chip with 3.4A10, only the antibody mixture which contained 6E10 did not increase the response level, while the antibody mixture which contained 4G8 or 12F4 could increase the response levels (>2000 IU) (Table 1). This data suggested that 3.4A10 competitively inhibited binding of 6E10 to the sensor chip and its epitope located in the N-terminal portion of $A\beta_{1-42}$ as 6E10 did.

3.4A10 had higher affinity to $A\beta_{1-42}$ than $A\beta_{1-40}$

Biacore affinity analyses were performed to measure the affinity of 3.4A10 to $A\beta_{1-40}$ and $A\beta_{1-42}$. The Biacore binding curves obtained using concentrations of 3.4A10 from 100 nM to 500 nM were analyzed assuming a one to one interaction by a BIAevaluation software. The dissociation constants (KD) of 3.4A10 to $A\beta_{1-40}$ and $A\beta_{1-42}$ were 3.77×10^{-8} M and 5.64×10^{-11} M, respectively (the χ^2 of the two analyses were 10.4 and 11.7, respectively) (Table 2). These data were consistent to the results of dot blot and western blot as well as the results of senile plaque staining as mentioned below.

Table 1
Biacore competitive epitope analysis of 3.4A10

	Cycle 1			Cycle 2			Cycle 3		
	baseline	3.4A10	with 6E10	baseline	3.4A10	with 4G8	baseline	3.4A10	with 12F4
Response level (RU)	3001.6	7937.8	7927.1	2750.5	8620.0	10684.6	2752.7	8602.4	10937.7

The $A\beta_{1-42}$ immobilized CM5 sensor chip was firstly saturated with 200 μg/ml 3.4A10 in PBS, then a 20:1 ratio antibody mixture (3.4A10: 6E10, 4G8 or 12F4) was injected and the response levels of each cycle were recorded. Results showed that 3.4A10 competed binding site with 6E10, as a result there was no increase in response levels after antibody mixture injection, while 3.4A10 did not compete binding site with 4G8 or 12F4, so after injection of antibody mixture, there was an increase in response levels (>2000 RU). The result suggests that the epitope of 3.4A10 exists in the same region as that of 6E10.

Table 2
Dissociation constant of 3.4A10 to $A\beta_{1-40}$ and $A\beta_{1-42}$

	$A\beta_{1-40}$	$A\beta_{1-42}$
Dissociation constant (KD)	3.77×10^{-8}M	5.64×10^{-11}M
χ^2	10.4	11.7

The Biacore binding curves obtained using concentrations of 3.4A10 from 100 nM to 500 nM were analyzed assuming a one to one interaction by BIAevaluation software. The data show that 3.4A10 has more affinity to $A\beta_{1-42}$ than to $A\beta_{1-40}$.

3.4A10 did not bind AβPP fragments

One of TAPIR antibody's features is that the antibody does not recognize both native and denature AβPP fragments. Western blot results showed that 3.4A10 did not recognize the denatured sAβPPα, immature AβPP and mature AβPP separated on SDS-PAGE from the lysate of human neuroblastoma SH-SY5Y cells transfected with wild type human AβPP, and mouse anti-AβPP A4 monoclonal antibody 22C11 was used as a positive control (Fig. 1D). To demonstrate that 3.4A10 did not bind native AβPP, a living cell staining was used. The results showed that 3.4A10 did not recognize the native AβPP that expressed on the surface of the cells (Fig.1E), while as a positive control 6E10 stained the cells (Fig. 1F).

3.4A10 inhibited $A\beta_{1-42}$ fibrillar aggregation and disaggregated pre-aggregated $A\beta_{1-42}$

To determine whether 3.4A10 has an effect on inhibition of $A\beta_{1-42}$ aggregation, 3.4A10/freshly prepared $A\beta_{1-42}$ was incubated at 1:10 molar ratio at 37°C for 1 week. 3.4A10 inhibited $A\beta_{1-42}$ aggregation to 36.7 ± 0.67% of the control (PBS only without antibody) by a thioflavin T fluorescence spectrophotometry assay (Fig. 2A). To elucidate the solubilization effect of 3.4A10 on $A\beta_{1-42}$, 3.4A10 was also incubated with pre-aggregated $A\beta_{1-42}$about 1:10 molar ratio at 37°C for 2 days, and the results of fluorescence spectrophotometry assay showed that 3.4A10 reduced 490 nm emission value of pre-aggregated $A\beta_{1-42}$ by 22.3 ± 3.48% compared to the control (Fig. 2B).

3.4A10 recognized less senile plaque core than 4G8

Consecutive AD brain sections were cut, and 3 pairs of the sections 100 μm apart were stained with 3.4A10 or 4G8. The 3.4A10 stained both classical and diffuse plaques in a similar pattern with 4G8, but only 7.5 ± 1.57% of the plaques had the core, while 4G8 stained the core in 14.93 ± 2.7% of the plaques ($P < 0.05$) (Fig. 3). To confirm this result, we stained another 3 pairs of the sections and got similar results (data not shown).

Therapeutic effects of 3.4A10

One mouse in the treatment group died after receiving 4 times injection due to an unknown reason. So at the end point of the experiment, 3 mice in the therapeutic group and 4 mice in the control group enrolled in further studies.

3.4A10 reduced the amyloid burden

The effect of 3.4A10 administration on development of an AD-like neuropathology in Tg2576 mice was investigated by a quantitative image analysis. Administration of 3.4A10 for 8 weeks resulted in marked reduction of amyloid burden in cortex and hippocampus compared with the control group (Fig. 4A). The mean value of amyloid burden in therapeutic group (cortex: 0.31 ± 0.09%, hippocampus: 0.59 ± 0.08%) was significantly reduced compared with the control group (cortex: 0.72 ± 0.23%, hippocampus: 0.99 ± 0.25%, $P < 0.05$) (Fig. 4B).

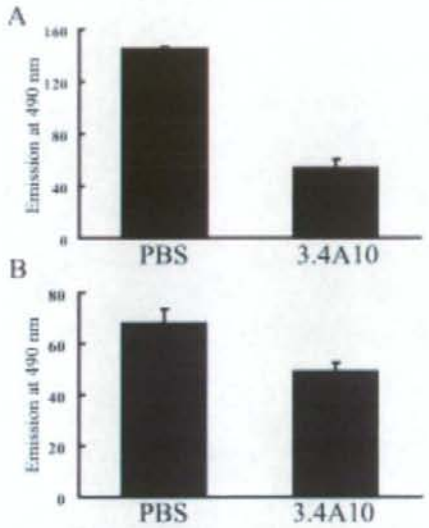

Fig. 2. 3.4A10 inhibited $A\beta_{1-42}$ fibrillation and degraded pre-aggregated $A\beta_{1-42}$ by thioflavin T-based fluorescence spectrophotometry. A) The freshly prepared 25 mM $A\beta_{1-42}$ in PBS was incubated with 2.5 mM 3.4A10 in a final volume of 25 μl at 37°C for 1 week, and 1 ml of 5 mM thioflavin T was added to the system and fluorescence was measured at an excitation wavelength of 445 nm and an emission wavelength of 490 nm. The results showed that 3.4A10 decreased the fluorescence to 36.7% ± 0.67% of the control. B) For degradation assay, 3.4A10 was incubated with pre-aggregated $A\beta_{1-42}$ about 1:10 molar ratio at 37°C for 2 days, and fluorescence spectrophotomtry assay showed that 3.4A10 reduced 490 nm emission value of pre-aggregated $A\beta_{1-42}$ by 22.3 ± 3.48% compared to the control. The figure shows the values (mean ± SD) of an example of similar results.

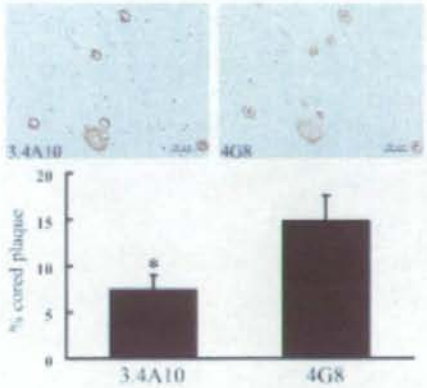

Fig. 3. 3.4A10 recognized less plaque cores than 4G8. Pairs of consecutive frozen sections of AD patient brain were stained with 1 μg/ml 3.4A10 or 4G8. 3.4A10 stained preferably the peripheral zone of senile plaques in the similar pattern with 4G8 and recognized less plaque cores compared with 4G8. The percentage of cored plaques was compared between 3.4A10 and 4G8 (7.5 ± 1.57% versus 14.93 ± 2.7%). Scale bar represents 100 μm. * $P < 0.05$.

The reduced amyloid burden was further confirmed by a quantitative ELISA measurement for the $A\beta_{42}$ and $A\beta_{40}$ contents in brain lysates. The results showed that $A\beta_{42}$ levels of the 3.4A10 therapeutic group in both SDS-soluble fraction and formic acid (non-soluble) fraction were decreased significantly compared with the control group (41.86 ± 2.64 nmol/g and 53.06 ± 4.99 nmol/g for SDS-soluble fraction of the therapeutic and the control group, respectively, $p = 0.017$; 682.91 ± 107.17 nmol/g and 1,040.40 ± 212.21 nmol/g for non-soluble fraction of the therapeutic and the control group, respectively, $p = 0.046$). While 3.4A10 therapy less interfered with the $A\beta_{40}$ levels compared to the control group (109.26 ± 39.91 nmol/g and 118.71 ± 13.89 nmol/g for SDS soluble fraction of the therapeutic and the control group, respectively, $p = 0.67$; 3,331.29 ± 2135.03 nmol/g and 5,485.44 ± 2620.58 nmol/g for non-soluble fraction of the therapeutic and the control group, respectively, $p = 0.30$) (Fig. 4C). The $A\beta$ oligomers in TBS fraction were detected by western blot. 3.4A10 therapy resulted in a reduction in the contents of $A\beta$*56 (12mer) compared to the control, while no apparent effects on other $A\beta$ oligomers (Supplementary Fig. 1).

No lymphocytic infiltration and no obvious increase of microhemorrhage in the brain of 3.4A10-treated mice

The lymphocytic infiltration was investigated in the brain of Tg2576 mice treated with 3.4A10 by staining with hematoxylin and eosin (HE) and by immunohistochemical staining with antibodies against CD3e and CD19, the markers of mature T-lymphocyte and B-lymphocyte, respectively. There were no histological or immunohistochemical differences in the brain sections between the therapeutic and the control groups (Fig. 5A–F).

The brain microhemorrhage is reported as an adverse side effect of passive immunotherapy in $A\beta$PP transgenic mice due to the increased vascular amyloid burden [25,26]. There was slightly increased microhemarrhage in the therapeutic group by counting the Berlin blue-positive blood vessels but it was not statistically significant (1.67 ± 1.17 versus 0.42 ± 0.21, $P = 0.27$). The Berlin blue-positive blood vessels of both groups were shown in Fig. 5G-H.

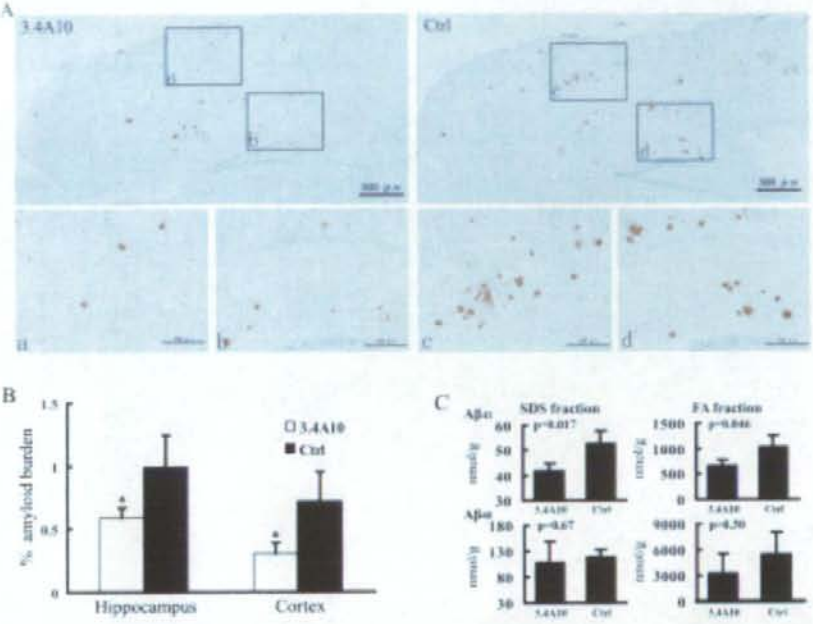

Fig. 4. 3.4A10 reduced the brain amyloid burden. A) Pan Aβ staining in sagittal brain sections showed that 3.4A10 therapy reduced the amyloid burden markly compared to the control. The upper two pictures represent the hippocampus and adjacent cortex of the 3.4A10 therapeutic and the control group in a low magnification and picture a-d represent the regions with more pronounced effect between the two groups. a, c: cortex; b, d: hippocampus, scale bar = 100 μm. B) The percentage of the area occupied by Aβ deposits in the brain section, which was determined by a quantitative image analysis. 3.4A10 therapy significantly reduced the amyloid burden in cortex and hippocampus compared to the control group. $^{*}P < 0.05$. C) The results of a quantitative ELISA for $A\beta_{40}$ and $A\beta_{42}$ contents in the SDS-soluble and formic acid fractions of the brain lysate. FA, formic acid. The 3.4A10 therapy significantly reduced $A\beta_{42}$ levels in both fraction and less interfered with $A\beta_{40}$ levels.

3.4A10 entered the brain and decorated some plaques which were surrounded with more Iba1-positive microglia

Alexa 594-labeled donkey anti-mouse IgG antibody was used to detect whether 3.4A10 could enter the brain. The immunofluorescence staining showed 3.4A10 entered the brain and the fluorescence (red) was co-localized with some of rabbit anti-pan Aβ antibody-detected senile plaques (green) (Fig. 6A upper panel). Alexa 594-labeled donkey anti-mouse IgG antibody did not stain any plaques in the control group (Fig. 6A lower panel).

Some plaques in the therapeutic group were surrounded by more Iba1-positive microglia, but the average number of microglia per plaque was not different between the two groups (data not shown). Then the average number of microglia was compared between 3.4A10-decorated and non-decorated plaques in the therapeutic group, the results showed that 3.4A10-decorated plaques were surrounded with more Iba1-positive microglia compared to the non-decorated plaques (9.28 ± 1.80 versus 5.43 ± 1.51, $p < 0.001$) (Fig. 6B–C).

Astrocytes were investigated by GFAP immunofluorescence staining. The results showed that there was no difference in GFAP-positive astrocytes between the two groups (Fig. 6D).

DISCUSSION

As one of key features of AD pathology, the extracellular amyloid deposits comprised of Aβ is a target of therapeutic approaches to AD, and the immunotherapies aimed at decreasing amyloid burden have been shown their effects on improvement of pathologic changes and cognitive functions in animals [1,5, 8,11,14,19,20,27] as well as in humans [7,10,21]. As

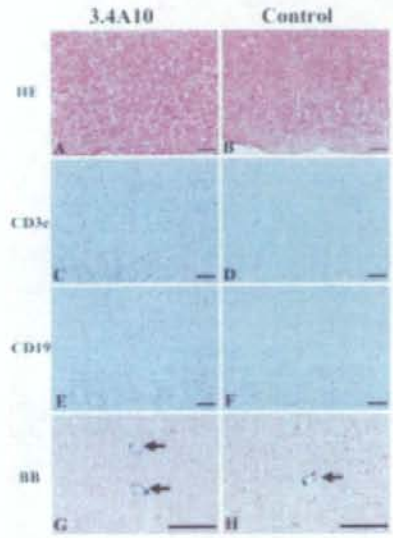

Fig. 5. No lymphocytic infiltration and slight but not significant increase of microhemorrhage in the brain sections. Staining with HE (A, B), Berlin blue (G, F) and antibodies against CD3e (C, D) and CD19 (E, F) in the sagittal brain sections of the Tg2576 mice. The arrows in G and F show the Berlin blue positive vessels. Left panel, 3.4A10 therapeutic group; right panel, control group. Scale bar = 100 μm. HE, hematoxylin and eosin stain; BB, Berlin blue stain.

one branch of immunotherapy, unlike active immunization, the passive immunization would not elicit undesired cellular responses, and more importantly, it allows us to monitor the antibody titer to modify the dosage and frequency of antibody infusion in order to avoid any adverse effects that might follow the passive administration of antibody without consideration whether the vaccine could arouse the immune response or not individually. Previous studies showed that anti-Aβ antibodies that effectively reduced amyloid burden had the following features: 1) ability to stain senile plaques rather than bind soluble Aβ; and 2) epitope location within N-terminus of Aβ [1,2,18]. Moreover, the TAPIR antibody was related to the slower decline of cognitive functions in AD patients who received active immunization [10].

The obtained anti-human Aβ mouse monoclonal antibody, 3.4A10, was selected by ELISA, but further immunohistochemical staining showed its ability to recognize senile plaques. The results of detection of Aβ fragments by 3.4A10 with dot blot and western blot simulated the patterns of anti-$Aβ_{1-42}$ C-terminal specific antibodies, however, the competitive Biacore analysis showed that 3.4A10 only blocked the binding of 6E10, an anti-Aβ N-terminal antibody, to the sensor chip without inhibiting the binding of other two antibodies that recognize the middle portion and C-terminal portion of Aβ. We concluded that epitope of 3.4A10 is located in the N-terminal portion of Aβ. And the ability of 3.4A10 to inhibit $Aβ_{1-42}$ aggregation on the ThT spectrophotometry assay further confirmed this conclusion as previously reported that N-terminal 3–6 amino acid residues EFRH of Aβ were presented as the epitope of its anti-aggregating antibodies [6]. More interestingly, 3.4A10 had higher affinity to $Aβ_{1-42}$ than to $Aβ_{1-40}$, and this was consistent with the dot blot and western blot results that 3.4A10 detected $Aβ_{1-42}$ better than $Aβ_{1-40}$, as well as the immunohistochemical staining results that 3.4A10 recognized less plaque cores which contained mainly $Aβ_{1-40}$ [17]. Similarly, we also found that 3.4A10 immunoreactivities were rarely co-localized with von Willebrand factor-positive blood vessels in AD brain samples (data not shown). We termed 3.4A10 as a TAPIR-like antibody due to above mentioned characteristics in addition to the fact that it did not recognize native or denatured AβPPs.

We also evaluated the therapeutic effects of 3.4A10 in a small number of 18 months old Tg2576. As expected, 3.4A10 significantly decreased the amyloid burden in brain after 8 weeks treatment by a quantitative image analysis. We also measured the $Aβ_{40}$ and $Aβ_{42}$ contents in the brain lysates by a sensitive sandwich ELISA assay. As 3.4A10 had more affinity to $Aβ_{42}$ than to $Aβ_{40}$, 3.4A10 significantly reduced the $Aβ_{42}$ levels compared to the control group, while less interfered with $Aβ_{40}$ levels. It was suggested that the extracellular soluble Aβ*56 (12mer), a 56-kD Aβ assembly impaired memory independently of plaques or neuron loss [16]. 3.4A10 therapy diminished the Aβ*56 levels in the soluble fraction of brain lysates by a western blot analysis.

The major adverse effect of passive anti-Aβ antibody therapy in the mouse model of AD is the increased incidence of microhemorrhage due to the age-related cerebral amyloid angiopathy (CAA) [25,26]. Tg2576 mouse model of AD carries Swedish mutation of AβPP under control of hamster prion protein promoter, and was found that $Aβ_{1-40}$ is the predominant amyloid deposit component [12]. The selective increase of $Aβ_{1-40}$ results in development of high levels of CAA and related cerebral microhemorrhage [25]. We investigated the microhemorrhage in the 3.4A10-treated mice and control mice, and found that there was slight but not significant increase in microhemorrhage.

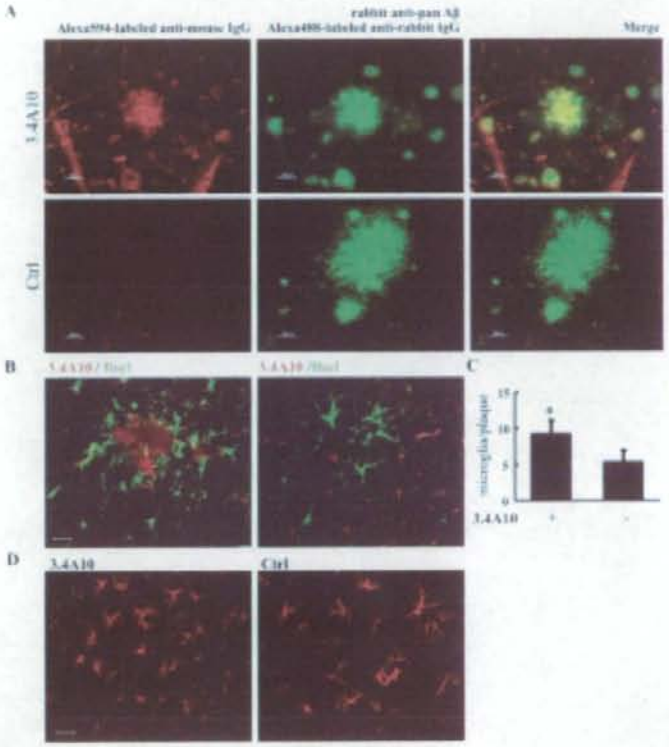

Fig. 6. 3.4A10 entered the brain and decorated some plaques which were surrounded with more Iba1-positive microglia. A) That 3.4A10 entered the brain was elucidated by direct staining of the sections with Alexa 594-labeled donkey anti-mouse IgG antibody. The 3.4A10 decorated plaques (red) were colocalized with rabbit anti-pan Aβ antibody stained ones (green) as shown in the upper panel of A. Alexa 594-labeled donkey anti-mouse IgG antibody did not stain any plaque in the brain sections of the control group as shown in lower panel of A. Bar = 25 μm. B) 3.4A10 decorated plaques (red) were surrounded more Iba1-positive microglia (green) than 3.4A10 negative plaques in the 3.4A10 therapeutic group, bar = 20 μm. C) The numbers of microglia per plaque were compared between 3.4A10 positive and negative plaques in the 3.4A10 therapeutic group. $^{*}p < 0.001$. D) There was no difference in GFAP-positive astrocytes between the two groups, bar = 20 μm.

This negative result may be due to the lower affinity of 3.4A10 to $A\beta_{1-40}$ and should be interpreted prudently. Meningoencephalitis was also reported to associate with passive immunization [15], but we did not see any inflammatory changes by HE staining and immunohistochemical staining for T and B lymphocytes.

There have been three hypotheses used to explain how antibodies reduced Aβ deposition [31]. One is that the direct effect of antibody on Aβ, leading to dissolution of amyloid fibrils [6,14,30]. The second hypothesis is that anti-Aβ antibody induces Fc receptor (FcR)-mediated phagocytosis of Aβ by microglia [1, 27]. The third one is termed as peripheral sink hypothesis, postulates that anti-Aβ antibody in the circulation leads to a net efflux of Aβ from brain to plasma [5]. Our results suggested that all of these three possible mechanisms might contribute to the decreased amyloid burden by 3.4A10 therapy. 3.4A10 degraded the $A\beta_{1-42}$ fibrils *in vitro*; 3.4A10 entered the brain and decorated some senile plaques which were surrounded by more Iba1-positive microglia; 3.4A10 therapy increased the serum $A\beta_{42}$ levels by a quantitative ELISA assay (data not shown).

Although the clinical trial was halted, Aβ immunotherapy would still be a potential therapeutic or preventive approach for AD. 3.4A10, the antibody we developed in this study, recognizes N-terminal portion of Aβ with a different affinity to Aβ species ($A\beta_{1-42}$ >

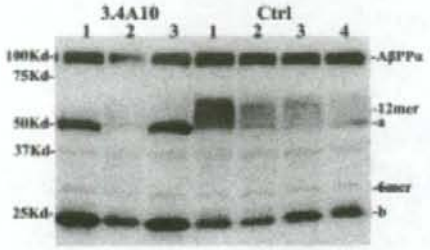

Fig. 7. Western blot results of Aβ oligomers in TBS fraction of the brain lysates. Compared to the control, the 3.4A10 reduced the 12mer Aβ oligomer without obvious effects on other Aβ oligomer. The sAβPP and amyloid oligomers were detected by 6E10 and HRP conjugated goat anti-mouse IgG second antibody. a, immunoglobulin heavy chain; b, immunoglobulin light chain.

$A\beta_{1-40}$), and more importantly it recognizes the senile plaques without binding the native or denatured form of AβPPs. The animal experiment showed its ability to decrease brain amyloid burden in a relatively short period (8 weeks) without any obvious side effects related to immunotherapy as previous reported. Further intensive study should be performed in order to provide some insights for selecting anti-Aβ antibodies for AD treatment.

ACKNOWLEDGMENTS

This work was supported in part by grand in aid for Scientific Research on Priority Area (17025056) from the Ministry of Education, Culture, Science and Technology. We Thank Dr. K. Takahashi, H. Wakida, A. Watanaba, A. Sekiyama, K. Takeda, K. Yoshizaki, K. Adachi and H.Y. Liu for their kind help and discussion in this work.

References

[1] F. Bard, C. Cannon, R. Barbour, R.L. Burke, D. Games, H. Grajeda, T. Guido, K. Hu, J. Huang, K. Johnson-Wood, K. Khan, D. Kholodenko, M. Lee, I. Lieberburg, R. Motter, M. Nguyen, F. Soriano, N. Vasquez, K. Weiss, B. Welch, P. Seubert, D. Schenk and T. Yednock, Peripherally administered antibodies against amyloid β-peptide enter the central nervous system and reduce pathology in mouse model of Alzheimer's disease, *Nat Med* **6** (2000), 916–919.

[2] F. Bard, R. Barbour, C. Cannon, R. Carretto, M. Fox, D. Games, T. Guido, K. Hoenow, K. Hu, K. Johnson-Wood, K. Khan, D. Kholodenko, C. Lee, M. Lee, R. Motter, M. Nguyen, A. Reed, D. Schenk, P. Tang, N. Vasquez, P. Seubert and T. Yednock, Epitope and isotype specificities of antibodies to beta-amyloid peptide for protection against Alzheimer's disease-like neuropathology, *Proc Natl Acad Sci USA* **100** (2003), 2023–2028.

[3] R. Bullock, Future directions in the treatment of Alzheimer's disease, *Expert Opin Investig Drugs* **13** (2004), 303–314.

[4] J.L. Cummings, Alzheimer's disease, *N Engl J Med* **351** (2004), 56–67.

[5] R.B. DeMattos, K.R. Bales, D.J. Cummins, J.C. Dodart, S.M. Paul and D.M. Holtzman, Peripheral anti-Aβ antibody alters CNS and plasma Aβ clearance and decreases brain Aβ burden in a mouse model of Alzheimer's disease, *Proc Natl Acad Sci USA* **98** (2001), 8850–8855.

[6] D. Frenkel, M. Balass and B. Solomon, N-terminal EFRH sequence of Alzheimer's β-amyloid pepetide represents the epitope of its anti-aggregating antibodies, *J Neuroimmunol* **88** (1998), 85–90.

[7] S. Gilman, M. Koller, R.S. Black, L. Jenkins, S.G. Griffith, N.C. Fox, L. Eisner, L. Kirby, M.B. Rovira, F. Forette and J.M. Orgogozo, AN1792(QS-21)-201 Study Team, Clinical effects of Abeta immunization (AN1792) in patients with AD in an interrupted trial, *Neurology* **64** (2005), 1553–1562.

[8] H. Hara, A. Monsonego, K. Yuasa, K. Adachi, X. Xiao, S. Takeda, K. Takahashi, H.L. Weiner and T. Tabira, Development of a safe oral Abeta vaccine using recombinant adeno-associated virusvector for Alzheimer's disease, *J Alzheimers Dis* **6** (2004), 483–488.

[9] C. Hock, U. Konietzko, A. Papassotiropoulos, A. Wollmer, J. Streffer, R.C. Von Rotz, G. Davey, E. Moritz and R.M. Nitsch, Generation of antibodies specific for β-amyloid by vaccination of patients with Alzheimer disease, *Nat Med* **8** (2002), 1270–1275.

[10] C. Hock, U. Konietzko, J.R. Streffer, J. Tracy, A. Signorell, B. Muller-Tillmanns, U. Lemke, K. Henke, E. Moritz, E. Garcia, M.A. Wollmer, D. Umbricht, D.J. de Quervain, M. Hofmann, A. Maddalena, A. Papassotiropoulos and R.M. Nitsch, Antibodies against beta-amyloid slow cognitive decline in Alzheimer's disease, *Neuron* **38** (2003), 547–554.

[11] C. Janus, J. Pearson, J. McLaurin, P.M. Mathews, Y. Jiang, S.D. Schmidt, M.A. Chishti, P. Horne, D. Heslin, J. French, H.T. Mount, R.A. Nixon, M. Mercken, C. Bergeron, P.E. Fraser, P. St George-Hyslop and D. Westaway, A beta peptide immunization reduces behavioural impairment and plaques in a model of Alzheimer's disease, *Nature* **408** (2000), 979–982.

[12] T. Kawarabayashi, L.H. Younkin, T.C. Saido, M. Shoji, K.H. Ashe and S.G. Younkin, Age-dependent changes in brain, CSF, and plasma amyloid β protein in the Tg2576 transgenic mouse model of Alzheimer's disease, *J Neurosci* **21** (2001), 372–381.

[13] H.W. Klafki, M. Staufenbiel, J. Kornhuber and J. Wiltfang, Therapeutic approaches to Alzheimer's disease, *Brain* **129** (2006), 2840–2855.

[14] I. Klyubin, D.M. Walsh, C.A. Lemere, W.K. Cullen, G.M. Shankar, V. Betts, E.T. Spooner, L. Jiang, R. Anwyl, D.J. Selkoe and M.J. Rowan, Amyloid β protein immunotherapy neutralizes Aβ oligomers that disrupt synaptic plasticity *in vivo*, *Nat Med* **11** (2005), 556–561.

[15] E.B. Lee, L.Z. Leng, V.M. Lee and J.Q. Trojanowski, Meningoencephalitis associated with passive immunization of a transgenic murine model of Alzheimer's amyloidosis, *FEBS Lett* **579** (2005), 2564–2568.

[16] S. Lesne, M.T. Koh, L. Kotilinek, R. Kayed, C.G. Glabe, A. Yang, M. Gallagher and K.H. Ashe, A specific amyloid-β protein assembly in brain impairs memory, *Nature* **440** (2006), 352–357.

[17] C.L. Master, G. Simms, N.A. Weinman, G. Multhaup, B.L. McDonald and K. Beyreuther, Amyloid plaque core protein in

Alzheimer disease and Down syndrome, *Proc Natl Acad Sci USA* **82** (1985), 4245–4249.

[18] J. Mclaurin, R. Cecal, M.E. Kierstead, X. Tian, A.L. Phinney, M. Manea, J.E. French, M.H. Lambermon, A.A. Darabie, M.E. Brown, C. Janus, M.A. Chishti, P. Horne, D. Westaway, P.E. Fraser, H.T. Mount, M. Przybylski and P. St George-Hyslop, Thearpeutically effective antibodies against amyloid-beta peptide target amyloid residues 4–10 and inhibit cytotoxicity and fibrillogenesis, *Nat Med* **8** (2002), 1263–1269.

[19] D. Morgan, D.M. Diamond, P.E. Gottschall, K.E. Ugen, C. Dichey, J. Hardy, K. Duff, P. Jantzen, G. DiCarlo, D. Wilcock, K. Connor, J. Hatcher, C. Hope, M. Gordon and G.W. Arendash, A beta peptide vaccination prevents memory loss in an animal model of Alzheimer's disease, *Nature* **408** (2000), 982–985.

[20] A. Mouri, Y. Noda, H. Hara, H. Mizoguchi, T. Tabira and T. Nabeshima, Oral vaccination with a viral vector containing Abeta cDNA attenuates age-related A beta accumulation and memory deficits without causing inflammation in a mouse Alzheimer model, *FASEB J* **21** (2007), 2135–2148.

[21] J.A. Nicoll, D. Wilkinson, C. Holmes, P. Steart, H. Markham and R.O. Weller, Neuropathology of human Alzheimer disease after immunization with amyloid-beta peptide: a case report, *Nat Med* **9** (2003), 448–452.

[22] R.L. Nussbaum and C.E. Ellis, Alzheimer's disease and Parkinson's disease, *N Engl J Med* **348** (2003), 1356–1364.

[23] J.M. Orgogozo, S. Gilman, J.F. Dartigues, B. Laurent, M. Puel, L.C. Kirby, P. Jouanny, B. Dubois, L. Eisner, S. Flitman, B.F. Michel, M. Boada, A. Frank and C. Hock, Subacute meningoencephalitis in a subset of patients with AD after Aβ42 immunization, *Neurology* **61** (2003), 46–54.

[24] R.L. Patton, W.M. Kalback, C.L. Esh, T.A. Kokjohn, G.D. Van Vickle, D.C. Luehrs, Y.M. Kuo, J. Lopez, D. Brune, I. Ferrer, E. Masliah, A.J. Newel, T.G. Beach, E.M. Gastano and A.E. Roher, Amyloid-β peptide remnants in AN-1972-immunized Alzheimer's disease patients, *Am J Pathol* **169** (2006), 1048–1063.

[25] M. Pfeifer, S. Boncristiano, L. Bondolfi, A. Stalder, T. Deller, M. Staufenbiel, P.M. Mathews and M. Jucker, Cerebral hemorrhage after passive anti-Aβ immunotherapy, *Science* **298** (2002), 1379.

[26] M.M. Racke, L.I. Boone, D.L. Hepburn, M. Parsadainian, M.T. Bryan, D.K. Ness, K.S. Piroozi, W.H. Jordan, D.D. Brown, W.P. Hoffman, D.M. Holtzman, K.R. Bales, B.D. Gitter, P.C. May, S.M. Paul and R.B. DeMattos, Exacerbation of cerebral amyloid angiopathy-associated microhemorrhage in amyloid precursor protein transgenic mice by immunotherapy is dependent on antibody recognition of deposited forms of amyloid β, *J Neurosci* **25** (2005), 629–636.

[27] D. Schenk, R. Barbour, W. Dunn, G. Gordon, H. Grajeda, T. Guido, K. Hu, J. Huang, K. Johnson-Wood, K. Khan, D. Kholodenko, M. Lee, Z. Liao, I. Lieberburg, R. Motter, L. Mutter, F. Soriano, G. Shopp, N. Vasquez, C. Vandevert, S. Walker, M. Wogulis, T. Yednock, D. Games and P. Seubert, Immunization with amyloid-β attenuates Alzheimer-disease like pathology in the PDAPP mouse, *Nature* **400** (1999), 173–177.

[28] D.J. Selkoe and D. Schenk, Alzheimer's disease: Molecular understanding predicts amyloid-based therapeutics, *Annu Rev Pharmacol Toxicol* **43** (2003), 545–584.

[29] B. Solomon, R. Koppel, E. Hanan and T. Katzav, Monoclonal antibodies inhibit in vitro fibrillar aggregation of Alzheimer β-amyloid peptide, *Proc Natl Acad Sci USA* **93** (1996), 452–455.

[30] B. Solomon, R. Koppel, D. Frankel and E. Hanan-Aharon, Disaggregation of Alzheimer β-amyloid by site-directed mAb, *Proc Natl Acad Sci USA* **94** (1997), 4109–4112.

[31] H.L. Weiner and D. Frenkel, Immunology and immunotherapy of Alzheimer's disease, *Nat Rev Immunol* **6** (2006), 404–416.

Tohoku J. Exp. Med., 2008, 215, 43-54

Juzen-taiho-to, an Herbal Medicine, Activates and Enhances Phagocytosis in Microglia/Macrophages

HUAYAN LIU,[1,2] JUN WANG,[1,2] ATSUO SEKIYAMA[1] and TAKESHI TABIRA[1]

[1]Department of Vascular Dementia Research, National Institute for Longevity Sciences, National Center for Geriatrics and Gerontology, Obu, Japan
[2]Department of Neurology, First Affiliated Hospital, China Medical University, Shenyang, P.R. China

Microglia are the main resident immunocompetent and phagocytic cells in the central nervous system (CNS). Activated microglia could play phagocytic roles as well as mediate inflammatory processes in the CNS. Involvement of activated microglia in the pathogenesis has been demonstrated in several neurological diseases including Alzheimer's disease (AD). Juzen-taiho-to (JTT), a traditional herbal medicine, has been reported to have effects on activating immune responses and phagocytosis. So far, little is known about the effects of this Kampo formulation JTT on microglia and in AD. In this report, we studied the effects of JTT on the activation and phagocytic functions of mouse microglia and bone marrow-derived macrophages (BMM). JTT could activate microglia, which was confirmed by the prominent morphological change and increased surface expression of an activation marker CD11b. In addition, JTT was revealed to induce microglial proliferation, and enhance microglial phagocytosis of, without eliciting an excessive production of nitric oxide. Furthermore, when mice were administrated with JTT in vivo, their BMM showed more effective phagocytosis of fibrillar $A\beta_{1\text{-}42}$. These findings implicate the therapeutic potential of JTT in AD and other neurological diseases accompanied by microglial activation. ——— Juzen-taiho-to (JTT); microglia/macrophages; Alzheimer's disease (AD); phagocytosis; amyloid.
Tohoku J. Exp. Med., 2008, **215** (1), 43-54.

Microglia are considered resident immune cells of myeloid origin, that take up residence in the central nervous system (CNS) during embryogenesis (Cuadros and Navascues 1998). They are regarded as CNS macrophages, and many studies gave evidence that immune reaction and inflammation related with microglia play essential roles in the pathological mechanism of some neurodegenerative diseases such as Alzheimer's disease (AD), multiple sclerosis, and so on (Rogers et al. 1988; Raine 1994). Activated microglia have been demonstrated to play the phagocytic role with extracellular β-amyloid deposits in AD (Kopec and Carroll 1998; Weldon et al. 1998). Therefore, microglia might be a therapeutic target for AD.

Juzen-taiho-to (Shi-Quan-Da-Bu-Tang in Chinese, JTT), a traditional herbal medicine, has traditionally been administered to patients with anemia, anorexia, or fatigue. From the pharmaco-

Received February 18, 2008; revision accepted for publication March 12, 2008.
Correspondence: Takeshi Tabira, National Institute for Longevity Sciences, National Center for Geriatrics and Gerontology, 36-3 Genko, Morioka, Obu 474-8511, Japan.
e-mail: tabira@nils.go.jp

logic view, JTT contains various immunomodulatory substances. For example, ginsenoside Rh1 has anti-allergic and anti-inflammatory activities (Park et al. 2004); glycyrrhizin extracted from Glycyrrhizae Radix and the extracts of Astragali Radix have anti-inflammatory activities (Shon and Nam 2003; Matsui et al. 2004); the extracts from Ginseng Radix, Cinnamomi Cortex, Glycyrrhizae Radix, Radix Paeoniae, and Astragali Radix have anti-oxidative activities (Dhuley 1999; Baltina 2003; Keum et al. 2003; Lee et al. 2003; Wang et al. 2003). Furthermore, recent studies demonstrated that ginsenosides Rg3 and Rh2 inhibited the production of nitric oxide (NO), iNOS and pro-inflammatory cytokines TNF-α, IL-1β in activated microglia (Bae et al. 2006). These results raised the possibility that the Kampo formulation JTT might have an immunomodulatory effect on microglia/macrophages, and might show its therapeutic potential in neurodegenerative diseases accompanied by microglial activation, such as AD.

In this study, we examined the effects of JTT on the activation and phagocytic functions of microglia and bone marrow-derived macrophages (BMM), as well as its effects on the production of NO in microglia.

Materials and Methods

Reagents

Synthetic human Aβ_{1-42} peptide was purchased from Peptide Institute, Inc. (Osaka). Fibrillar Aβ_{1-42} (fAβ_{42}) was obtained by dissolving the synthetic human peptide firstly in DMSO and then in Dulbecco's PBS (250 μM) followed by incubating at 37°C for 7 days. Lipopolysaccharide (LPS) from Escherichia coli 055: B5 was purchased from Sigma-Aldrich (St. Louis, MO, USA). Fluorescein isothiocyanate (FITC)-conjugated rat anti-mouse CD11b monoclonal antibody was purchased from BD Biosciences Pharmingen (San Jose, CA, USA). Rabbit anti-Iba1 (ionized calcium binding adaptor molecule 1) polyclonal antibody was purchased from Wako Pure Chemicals Industries, Inc. (Osaka). Mouse anti-human Aβ monoclonal antibody: 4G8 was purchased from Chemicon International, Inc. (Temecula, CA, USA). Rabbit anti-Lysosome-associated membrane protein (LAMP)-2 polyclonal antibody was purchased from Santa Cruz Biotechnology, Inc. (Santa Cruz, CA, USA). Recombinant mouse granulocyte macrophage-colony stimulating factor (GM-CSF) and recombinant mouse macrophage-colony stimulating factor (M-CSF) were from R & D Systems (Minneapolis, MN, USA).

Preparation of JTT

JTT, purchased from Tsumura and Co. (Tokyo), was composed of 10 medical plants (Table 1). JTT was prepared as follows. A mixture of Astragali Radix (3.0 g), Cinnamomi Cortex (3.0 g), Angelicae Radix (3.0 g), Paeoniae Radix (3.0 g), Cnidii Rhizoma (3.0 g), Rehmanniae Radix (3.0 g), Ginseng Radix (3.0 g), Atractylodis Lanceae Rhizoma (3.0 g), Poria (3.0 g), and Glycyrrhizae Radix (1.5 g) was added to 285 ml of water and extracted at 100°C for 1 hr. The extracted solution was filtered and spray-dried to obtain the dry extract powder (2.3 g).

Table 1. The ratio of crude drugs of Juzen-taiho-to (JTT)

Crude drugs	Ratio
Astragali Radix (*root of Astragalus membranaceus Bunge*)	3.0
Cinnamomi Cortex (*bark of Cinnamomum cassia Blume*)	3.0
Angelicae Radix (*root of Angelica acutiloba Kitagawa*)	3.0
Paeoniae Radix (*rhizome of Paeonia lactiflora Pallas*)	3.0
Cnidii Rhizoma (*rhizome of Cnidium officinale Makino*)	3.0
Rehmanniae Radix (*root of Rehmannia glutinosa Liboschitz var. purpurea Makino*)	3.0
Ginseng Radix (*root of Panax ginseng C.A. Meyer*)	3.0
Atractylodis Lanceae Rhizoma (*rhizome of Atractylodes lancea De Candolle*)	3.0
Poria (*scletrotium of Poria cocos Wolf*)	3.0
Glycyrrhizae Radix (*root of Glycyrrhiza uralensis Fischier*)	1.5